NOTIONAL SHIELDING FOR PULSED POWER IN COMBAT SYSTEMS

Alex E. Zielinski,* Ira Kohlberg,† John Bennett,‡ Calvin D. Le,§ and W. Jim Sarjeant**

Abstract

A model was developed for determining the space and time behavior of the magnetic field external to a system of conductors. A moving conductor is in relative close proximity to a stationary conductor that provides the source current. An additional conductor provides attenuation of the environmental field. The space and time periodicity of the field is related to the parameters of the system. A numerical example predicts the magnitude of the magnetic field as a function of distance from the stationary conductor. Initial shielding considerations for mitigating the environmental effects produced by this class of emerging technologies are developed. The assessment indicates that conventional engineering design, based on the principals of electromagnetic compatibility (EMC), can reduce the magnetic fields to levels consistent with the notional requirements of electric combat vehicles.

Introduction

Over the years, there has been continuing interest in the development of pulsed-power energy sources and accelerators based on the processes of transient magnetic field exclusion and diffusion. An essential feature of these devices involves a stationary source current and the generation of induced currents (i.e., eddy currents) in a moving finite conductivity conductor. The source and eddy currents produce magnetic fields that have a characteristic magnitude and frequency external to their geometry. Applications utilizing this process can be found in electromagnetic braking of large electromechanical systems [1, 2] and the generation of high electrical power pulses [3–5].

As these electrical devices mature into components for military systems, the electromagnetic compatibility (EMC) issues that arise from the environmental electric and magnetic fields they generate must be considered. Environmental fields are those fields that are created in spatial locations that are not especially close to the source and are concurrently located in close proximity to electronic equipment that may be affected. For example, environmental electromagnetic fields generated by capacitor-driven pulsed-power sources raise important EMC considerations for electromagnetic railguns [6, 7]. Superconducting electrical generators utilizing liquid metal slip-rings are also adversely affected by the influence of the magnetic operating environment [8]. Fortunately, standard shielding techniques, using conducting materials, are adequate for managing magnetic fields less than *1 T* [9]. For large confined fields, active shielding techniques can be more efficiently implemented [8, 9].

This paper discusses the results of a system of three conductors: namely a source, a moving conductor located in close proximity, and an environmental shield located some distance removed from the source. The magnetic induction field is of primary interest. Theoretical considerations are discussed, and a system model is developed. The environmental field calculated from the theoretical assessment is used to illustrate the design of an environmental shield with realistic material properties. Finally, the summary and conclusions are presented.

* U.S. Army Research Laboratory, Aberdeen Proving Ground, MD 21005-5066

† Kohlberg Associates Inc, PO Box 23077, Alexandria, VA 22304

‡ TACOM-ARDEC, Picatinny Arsenal, NJ 07806-5000

§ U.S. Army Research Laboratory, Adelphi, MD 20783-1197

** University of Buffalo – SUNY AB, PO Box 601900, Buffalo, NY 14260-1900

Report Documentation Page

Report Date	Report Type	Dates Covered (from... to)
27MAR2001	N/A	27MAR2001 - 29MAR2001

Title and Subtitle Notional Shielding for Pulsed Power in Combat Systems	**Contract Number**
	Grant Number
	Program Element Number
Author(s) Zielinski, Alex E.; Kohlberg, Ira; Bennett, John; Le, Calvin D.; Sarjeant, W. Jim	**Project Number**
	Task Number
	Work Unit Number
Performing Organization Name(s) and Address(es) US Army Research Laboratory Aberdeen Proving Ground, MD 21005-5066	**Performing Organization Report Number**
Sponsoring/Monitoring Agency Name(s) and Address(es) OSD Pentagon Washington, DC	**Sponsor/Monitor's Acronym(s)**
	Sponsor/Monitor's Report Number(s)

Distribution/Availability Statement
Approved for public release, distribution unlimited

Supplementary Notes
Papers from the Proceedings AIAA 2nd Biennial National Forum on Weapon System Effectiveness, held at the John Hopkins University/Applied Physics Laboratory, 27-29 March 2001. Controlling Agency is OSD, Pentagon, Washington DC, per Richard Keith, Editor. See also ADM201408, non-print version (whole conference).

Abstract

Subject Terms

Report Classification unclassified	**Classification of this page** unclassified
Classification of Abstract unclassified	**Limitation of Abstract** SAR

Number of Pages
10

Theoretical Considerations

The purpose of this study is to characterize the salient features of the environmental magnetic field generated by a spatially periodic time-varying source current. Figure 1 shows a close-up of the relationship between the spatially periodic source currents and a moving conductor. Previous work has shown that image theory was applicable to this type of problem with further simplification resulting from assuming infinite conductivity for the moving conductor [10]. This work also shows that for velocities greater than *100 m/s* and good conductivity for the moving conductor, the field contribution due to motion can be neglected.

Model Formalism

Figure 2 shows the geometry used for determining the ambient magnetic field in the presence of an environmental shield. It is assumed that both the moving conductor and the environmental shield have infinite conductivities and that they can be represented as an array of images. The system is assumed to be periodic and infinite in the $\pm x$ directions. Image theory permits the field in the space between the planes $y = 0$ and $y = -D$ to be computed by summing the fields due to the actual physical source and its images [10].

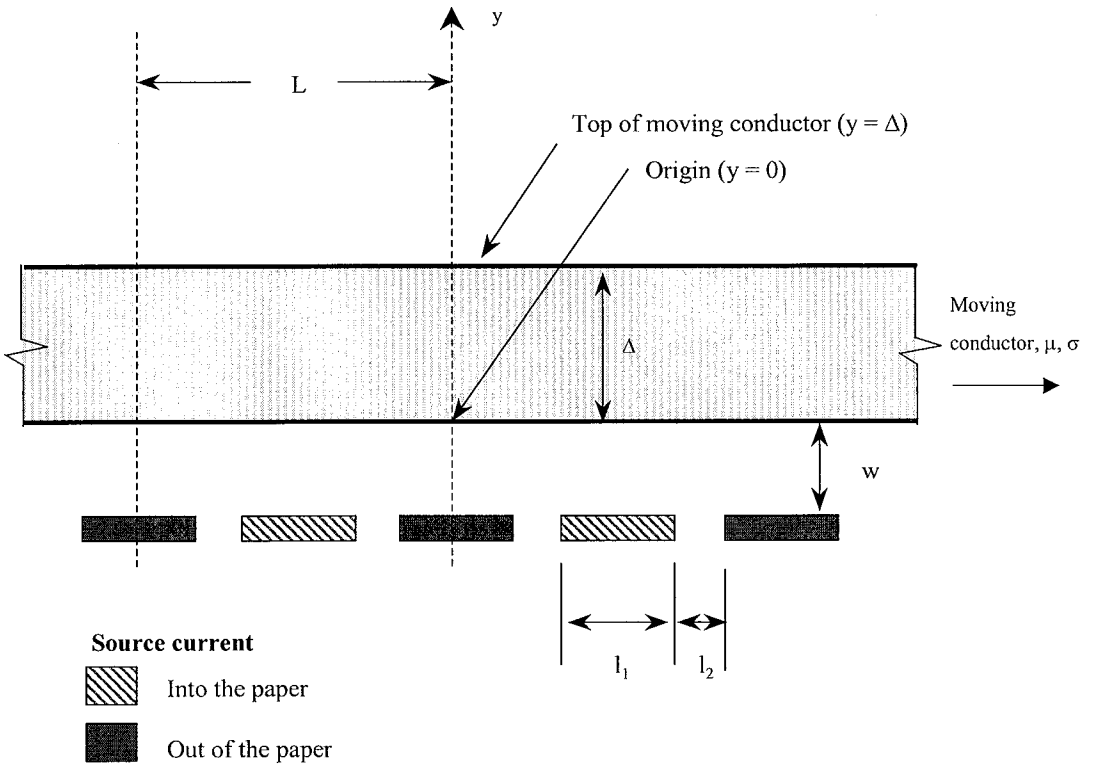

Figure 1. Source Current Elements and Moving Conductor.

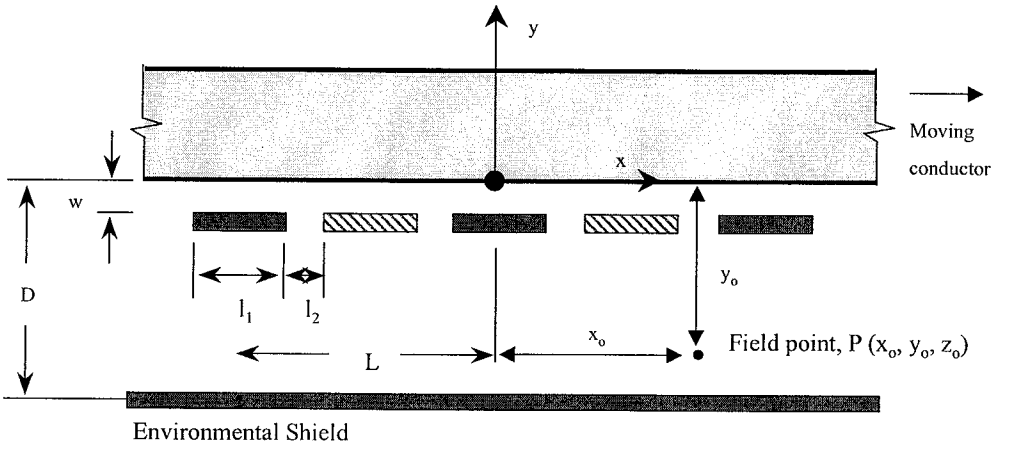

Front View

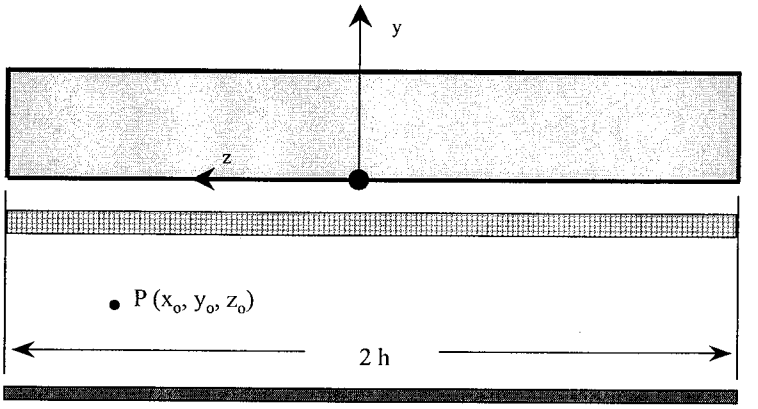

Side View

Figure 2. Geometric Considerations for Determining the Magnetic Field Produced by a Moving Conductor and Environmental Shield System.

The discontinuous linear current density, $\vec{J}_R$, of the periodic distribution of source elements shown in Figure 2 can be written as $\vec{J}_R = \vec{k}J_R$. The magnitude is

$$J_R(x,t) = A_J(t)\sum_{n=1}^{\infty} a_n \cos\frac{2n\pi x}{L}, \qquad (1)$$

where the characteristic length is $L = 2(l_1 + l_2)$ and the a_n's are determined from the orthogonality properties of the Fourier series. Using the discontinuous distributions

$$J_R(x) = A_J \ :\frac{l_1}{2} \geq |x| \geq 0,$$

$$= 0 \ :\frac{l_1}{2} + l_2 \geq |x| \geq \frac{l_1}{2},$$

and

$$= -A_J : l_1 + l_2 \geq |x| \geq \frac{l_1}{2} + l_2, \qquad (2)$$

where A_J is a constant, we derive

$$a_n = \frac{2}{n\pi}(1 - \cos n\pi)\sin\frac{n\pi l_1}{L}. \qquad (3)$$

The environmental magnetic field is computed for the region below the source conductors, that is, for field points satisfying the

condition $y_O < -w$. The two-dimensional form of the Biot-Savart law is given by

$$\vec{B}(\vec{r}_o) = \frac{\mu_o}{4\pi} \iint \frac{\vec{J}(\vec{r}) \times (\vec{r}_o - \vec{r})}{|\vec{r}_o - \vec{r}|^3} dxdz, \quad (4)$$

where the position vector is given by

$$\vec{r}_o = \vec{i}x_o + \vec{j}y_o + \vec{k}z_o. \quad (5)$$

When only the real source and its image are considered, the magnetic field at $\vec{r}_O$ is given by

$$\vec{B}(\vec{r}_o) = \vec{B}_R(\vec{r}_o) + \vec{B}_I(\vec{r}_o), \quad (6)$$

where $\vec{B}_R$ and $\vec{B}_I$ are the contributions from the real and image sources, respectively, and $\vec{B}_R$ is given by

$$\vec{B}_R = \frac{\mu_o}{4\pi} \int_{-\infty}^{+\infty} \int_{-h}^{+h} \frac{\vec{k}dz \times \vec{r}_R}{|\vec{r}_R|^3} J_R(x)dx. \quad (7)$$

The integration over x extends from $-\infty$ to $+\infty$, the integration over z extends from $-h$ to $+h$, and

$$\vec{r}_R = \vec{i}(x_o - x) + \vec{j}(y_o + w) + \vec{k}(z_o - z). \quad (8)$$

The foregoing expression simplifies when the observation point is located at the intersection of the midplanes $x_O = 0$ and $z_O = 0$. The integration with respect to z in equation (7) then yields for the contribution due to the source current

$$\vec{B}_R = -\vec{i}\frac{\mu_o}{4\pi}(y_o + w) \int_{-\infty}^{+\infty} J_R \frac{2h}{(x^2 + (y_o + w)^2)(h^2 + x^2 + (y_o + w)^2)^{1/2}} dx \quad (9)$$

Simplification results when the foregoing equations are cast in dimensionless form by introducing the variables

$$\rho = \frac{x}{L} \quad (10)$$

and

$$\eta = \frac{y_o + w}{L} \quad (11)$$

and selecting a specific value for h. For convenience, a value of $h = L$ is used. Inserting equation (1) into equation (9) and dropping the vector notation, gives

$$B_R = -\frac{\mu_o}{4\pi} A_J \sum_{n=1}^{n=\infty} a_n P_n(\eta), \quad (12)$$

where

$$P_n = 4\eta \int_0^{\infty} \frac{\cos 2n\pi\rho}{(\eta^2 + \rho^2)(1 + \eta^2 + \rho^2)^{1/2}} d\rho \approx 2\pi e^{-2n\eta} \quad (13)$$

for $\eta \geq 0$.

We also have

$$P_n(-\eta) = -P_n(\eta), \quad (14)$$

which is relevant since y_O is negative.

The total magnetic field, B_{net}, in terms of the source contribution, is computed from the formalism of equations (12–14), where the argument η of B_R is replaced by $(\eta + \frac{2mD}{L})$ and $(\eta - \frac{2w}{L} + \frac{2mD}{L})$ for all integer values of m, to reflect the contribution due to the image currents. Thus,

$$B_{net} = \sum_{m=-\infty}^{m=+\infty} \left[B_R(\eta + \tfrac{2mD}{L}) - B_R(\eta - \tfrac{2w}{L} + \tfrac{2mD}{L}) \right] \quad (15)$$

and the negative sign in front of the second term on the right accounts for the fact that these image currents are the negative of the real current.

Numerical Results

The purpose of this section is to obtain numerical estimates of the magnetic flux density as a function of vertical distance from the source conductor system for a particular set of parameters. The values listed in Table 1 are used throughout the paper, unless otherwise noted.

Table 1. Assumed Values for Numerical Calculations.

Conductor Width	l_1 (*mm*)	*250*
Conductor Spacing	l_2 (*mm*)	*100*
Characteristic Length	L (*m*)	*0.7*
Air Gap	W (*mm*)	*5*
Conductor Depth	h (*m*)	L
Peak Source Current	I_o (*MA*)	*1*

Using the numbers provided in Table 1 and noting from equation (3) that $a_n=0$ for n = even numbers yields $a_1 = 1.15$ and $a_3 = -0.094$. Subsequent values of a_n are negligible. Moreover, when a_1 and a_3 are combined with the evaluation of equation (13), the third harmonic is less than *10%* of the first harmonic. Hence, with very good approximation, reasonably accurate results are developed for $n=1$. Similarly, m in equation (15) is taken from -2 to $+2$.

For an environmental shield located some distance from the source, the eddy currents induced in the shield have very little influence on the flux density generated by the current source. However, as the shield is positioned in relative close proximity to the source current, the flux density at the source is decreased due to the eddy currents that produce a magnetic field in the vicinity of the source in opposition to the field generated by the source. Generally, a large flux density in the air gap is desired in order to maintain good coupling between the source and moving conductor. If the application is electromagnetic braking, then the distance required to reduce the conductor velocity to zero will be increased due to the smaller flux density. If the application is a power source, then the generated voltage will be less, again due to the reduced flux density. In Figure 3, the source current (normalized to the current required to maintain the same flux density in the absence of an environmental shield) is plotted as a function of the location of the environmental shield. The distance is normalized to the characteristic length. The plot includes three different values for the air gap (w). For a small air gap, as is required for efficient electromagnetic coupling, the location of the shield has a negligible effect on increasing the source current. For larger air gaps, generally used because of structural requirements on the conductors, the increase in source current is somewhat larger.

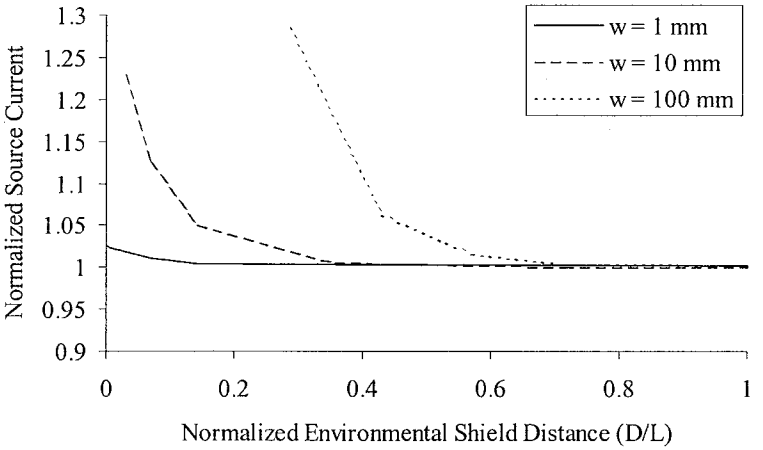

Figure 3. Normalized Source Current as a Function of Environmental Shield Location.

For example, a *10-mm* air gap and an environmental shield located *50 mm* from the source yields a *12%* increase in the source current or, alternatively, a *24%* increase in ohmic losses, an appreciable effect on the conductor system configured as either a load or generator.

For this study, the shield is placed at a sufficient distance from the source so as not to affect the flux density produced in the air gap, yet it is close enough to the source to demand reasonable attenuation from an environmental shield. The shield located at *D=200 mm* (*D/L=0.29*) meets this requirement.

Using the values from Table 1, the magnetic field is computed in Figure 4 as a function of distance from the source. At the source ($\eta = 0$), the induction field is *5.5 T*. Also shown in the figure is the magnetic field for the case where no environmental shield is included. In both cases, the magnetic field decays as a function of increasing distance from the source. The linear rate of decay is roughly *1 T/m*. However, the field is slightly larger in the region of space between the source and shield for the case with an environmental shield. The field incident on the shield is *0.092 T*, which is not an exorbitant quantity, but is sufficient to cause some EMC issues [9]. By definition, the field on the opposite side of the perfectly conducting shield is zero.

Environmental Shield Design

In the previous section, the environmental field in the region of space beyond the perfectly conducting shield was zero. In this section, the details of a finite conductivity shield are discussed. Experimentally obtained data characterizing the shield materials are used to quantify the design [9].

For a realistic environmental shield, the field beyond the shield will not be zero, but rather a small value. Small is a subjective term, but in this case is taken to be several orders of magnitude below the flux density generated in the air gap. For EMC considerations, the susceptibility of electronic components is evaluated as a function of the environmental field. This evaluation is complex and is very specific to the type of electronic components and their relative location to the source field. In the case of superconducting electrical machinery, the environmental magnetic field can cause unacceptable viscous and ohmic losses in the liquid-metal current collection system [8]. Sufficient attenuation of the field can reduce the losses to acceptable levels. In order to illustrate the present design analysis, however, a more simple exposure guideline, as determined by the American Conference of Governmental Industrial Hygienists (ACGIH), is used. The ACGIH threshold limit value (TLV) for

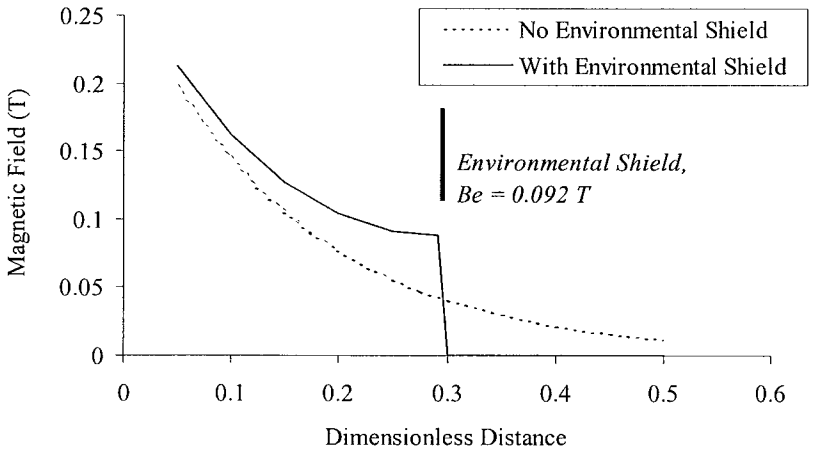

Figure 4. Magnetic Field as a Function of Dimensionless Distance (η).

exposure to a cyclical magnetic field is given by [11]

$$B_{TLV} = \frac{0.06}{f}, \qquad (16)$$

where f is the frequency of oscillation for the magnetic field.

Numerous nomenclature are used to describe the attenuation of magnetic fields. In this study, experimental results are adapted from the literature that describe the attenuation as the ratio of the peak incident field (*Be*) to the peak attenuated field (*Bi*), or magnetic shielding effectiveness (MSE), as a function of different materials and thicknesses [9]. Typically, the MSE is complex; however, only the magnitudes are considered. For magnetic materials, MSE is a function of the induction field since the permeability is dependent on the induction field.

A multilayer shield model is illustrated in Figure 5. Using a fit to the MSE of the form

$$MSE = ZB_o^c + 1, \qquad (17)$$

where B_o is the incident field (i.e., $Be=B_o$ for a single-layer shield), and the material constants Z and c are listed in Table 2. For the magnetic materials, the MSE is nearly *1* at a peak induction field of roughly *0.14 T* (i.e., saturation). For the copper material, the MSE is nearly constant for all field levels, and any deviation is attributable to the accuracy of the measurements and subsequent fit to the data.

The MSE discussed thus far is somewhat dependent on the waveform of the incident field. The constants listed in Table 2 correspond to the exposure field shown in Figure 6. Also shown in the plot is the attenuated field for an 8-layer shield (*2 mm* total thickness) constructed from TI-Shield (a copper, Permalloy 49 composite). The exposure field has a peak of *0.11 T* at a time of *0.46 ms*, which corresponds to a frequency of *543 Hz*. It can be seen that while the magnitude of the attenuated field is reduced to *0.06 T*, the rise to peak is now increased to *0.82 ms*. The rate of decay is slightly smaller for the attenuated field than for the exposure field.

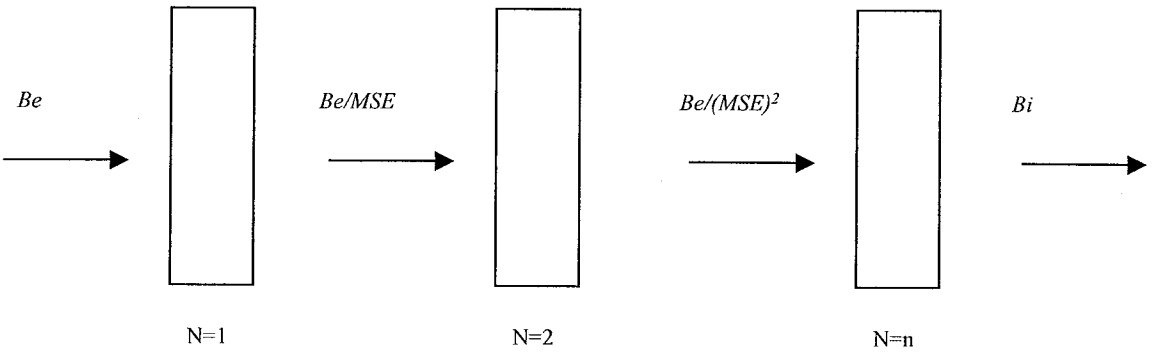

Figure 5. Illustration of Multilayer Shield Model.

Table 2. Fitting Constants for *0.25-mm*-thick Shield Materials [9].

Material	*c*	*Z*
Copper	*-0.7604*	*0.0065*
TI-Shield	*-1.4942*	*0.0017*
Mμ-Shield	*-1.2401*	*0.0026*

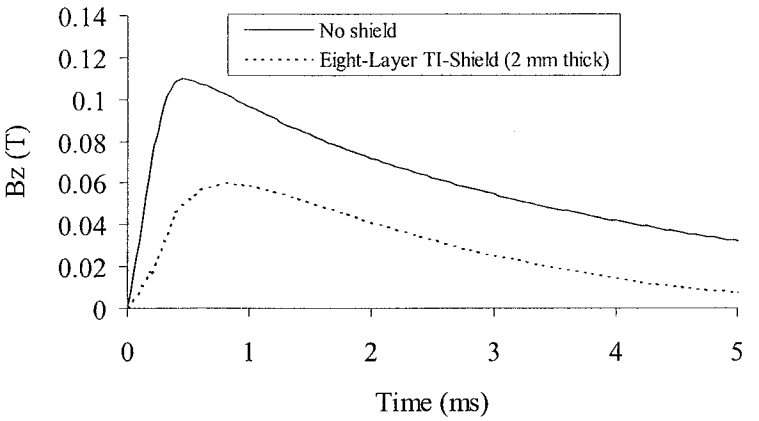

Figure 6. Measured Magnetic Induction Field as a Function of Time.

Finally, the geometry of the experiment and shield configuration can also effect the MSE. The constants listed in Table 2 were obtained for a cylindrical shield located in the bore of a railgun. The cylinders were open at both ends and were relatively short, having a ratio of length to diameter of about *1.2*. Additional data taken with one end of the cylinder closed increased the MSE by roughly *25%*. The corrected MSE data correlate very well to a calculation for the skin depth for an incident field at the surface of a flat-plate conductor. However, no attempt was made to adjust the constants listed in Table 2 to correspond to a flat-plate configuration.

The multilayer model illustrated in Figure 5, along with the material constants listed in Table 2, was used to successfully predict the attenuated field in the bore of a railgun. Some disparity between theory and experiment was obtained for the number of layers greater than *5*. This was attributed to the outermost layers in close proximity to the rail conductors, which carried a small amount of current and thereby canceled a portion of the shielded flux. This effect was not modeled.

The attenuated magnetic field just beyond the environmental shield is shown in Figure 7 as a function of total shield thickness. The constants listed in Table 2 were used with the multilayer shield model. The incident field (*Be = 0.092 T*) is taken from Figure 4 at the location of the environmental shield (*D = 200 mm*). For this level of incident field, there is very little difference in attenuation between the copper and magnetic materials for a total shield thickness of *5 mm*. As expected, the copper shield provides a near-linear attenuation of the field as a function of shield thickness. An aluminum shield would yield similar results. The Mμ–Shield material performs slightly better than the copper shield. The TI-Shield material, comprised of copper, Permalloy 49, and copper, performs even better, providing the largest attenuation for the thinnest shield.

Roughly *60 db* of attenuation is provided for *15 mm* of total shield thickness. Also indicated on the plot is the ACGIH TLV (*~0.1 mT*) corresponding to a frequency of *543 Hz*. The parameters listed in Table 1 correspond to a conductor moving at a velocity of *380 m/s*, well within the limits of the assumption for perfect conductors. Although not indicated in the plot, the attenuated field will also decay (barring the inclusion of any other source of electromagnetic radiation) as the distance from the shield is increased. Finally, the data presented in Figure 6 also suggest that the frequency of the attenuated field will be somewhat lowered, thereby adding complexity to any additional EMC requirements.

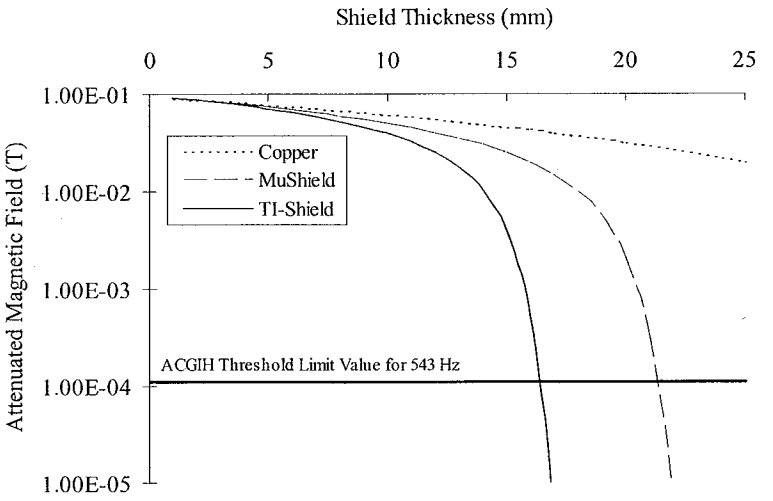

Figure 7. Attenuated Induction Field as a Function of Environmental Shield Thickness.

Summary and Conclusions

A model has been developed for determining the space and time behavior of the magnetic field external to a system of conductors. The model includes a moving conductor in relative close proximity to a stationary (source) conductor and an environmental shield. The analysis indicates that the magnetic field has a space and time periodicity that can be related to the parameters of the conductors. Furthermore, a numerical example is presented that predicts the magnitude of the magnetic induction field as a function of distance from the stationary conductor. In this analysis, the induced currents in the environmental shield, placed in relative close proximity to the source, can reduce the flux density at the source. The corresponding increase in the source current can be appreciable (i.e., > *25%*) for all but the most efficiently coupled conductors (i.e., small air gap). The environmental magnetic field decays to a manageable level at distances that produce a negligible effect on the source.

A composite shield design was found to efficiently attenuate the field produced by the conductor system to acceptable levels. The multilayer, *0.25-mm*-thick TI-Shield provided *60 db* of attenuation for roughly *15 mm* of total thickness. TI-Shield can be better utilized when field levels have been reduced to less than *0.06 T*. Specific exposure limits related to EMC were not available; however, the attenuated field is within the exposure guidance prescribed by ACGIH. While no attempt was made to include materials normally found on vehicles, there is no reason to suspect that existing metallic structures (i.e., steel) cannot be used to provide initial attenuation to *0.06 T*.

References

1. Bennett J., T. Gora, P. Kemmey, and W. Kolkert. "Electromagnetic Braking of a Metallic Projectile in Flight." *IEEE Transactions on Magnetics*, vol. 21, no. 3, May 1985.

2. Doyle, M. R., D. Samuel, T. Conway, and R. Klimowski. "Electromagnetic Aircraft Launch Systems - EMALS." *IEEE Transactions on Magnetics*, vol. 31, no. 1, pp. 528-533, January 1995.

3. Summerfield, M. "Development of a Linear Piston-Type Pulse Power Electric Generator for Powering Electric Guns." *IEEE Transactions on Magnetics*, vol. 29, no. 1, January 1993.

4. Kilgore, L. A., E. Hill, and C. Flick. "A New Three Million KVA Short Circuit Generator." *IEEE Transactions (Power Apparatus and Systems)*, no. 67, pp. 442-445, August 1963.

5. Pratap, S., and M. Driga. "Compensation in Pulsed Alternators." *IEEE Transactions on Magnetics*, vol. 35, no. 1, pp. 372-377, January 1999.

6. Kohlberg, I., C. Le, and A. Zielinski. "Predictions and Observations of Transient Electric and Magnetic Fields Generated by Electromagnetic Launch Systems." Conference Paper, XXVII International Union of Radio Science (URSI) General Assembly, Lille, France, 28 August-September, 1996.

7. Zielinski, A. E., C. Le, J. Bennett, and I. Kohlberg. "Railgun Electric Fields: Experiment and Theory." *IEEE Transactions on Magnetics*, vol. 31, no. 1, pp. 463, January 1999.

8. Bumby, J. R. *Superconducting Rotating Electrical Machines.* Department of Engineering, University of Durham, Oxford: Clarendon Press, 1983.

9. Zielinski, A. E. "In-Bore Magnetic Field Management." ARL-TR-1914, U.S. Army Research Laboratory, Aberdeen Proving Ground, MD, March, 1999.

10. Kohlberg, I., A. E. Zielinski, and C. Le. "Transient Electromagnetic Fields Produced by Pulsed Moving Conductors." ARL-TR-1931, U.S. Army Research Laboratory, Aberdeen Proving Ground, MD, April 1999.

11. Hitchcock, R. T., and R. M. Patterson. *Radio-Frequency and ELF Electromagnetic Energies: A Handbook for Health Professionals.* American Conference of Governmental Industrial Hygienists (ACGIH) Publication 9525, 1995.